

# Tuning the electronic properties of C12A7 via Sn doping and encapsulation

Kuganathan, N. & Chroneos, A.

Published PDF deposited in Coventry University's Repository

**Original citation:**

Kuganathan, N & Chroneos, A 2020, 'Tuning the electronic properties of C12A7 via Sn doping and encapsulation', Journal of Materials Science: Materials in Electronics, vol. (In-press), pp. (In-press).

<https://dx.doi.org/10.1007/s10854-020-04633-8>

DOI 10.1007/s10854-020-04633-8

ISSN 0957-4522

ESSN 1573-482X


Publisher: Springer

**Open Access** This article is licensed under a Creative Commons Attribution 4.0 International License, which permits use, sharing, adaptation, distribution and reproduction in any medium or format, as long as you give appropriate credit to the original author(s) and the source, provide a link to the Creative Commons licence, and indicate if changes were made. The images or other third party material in this article are included in the article's Creative Commons licence, unless indicated otherwise in a credit line to the material. If material is not included in the article's Creative Commons licence and your intended use is not permitted by statutory regulation or exceeds the permitted use, you will need to obtain permission directly from the copyright holder. To view a copy of this licence, visit <http://creativecommons.org/licenses/by/4.0/>.

Copyright © and Moral Rights are retained by the author(s) and/ or other copyright owners. A copy can be downloaded for personal non-commercial research or study, without prior permission or charge. This item cannot be reproduced or quoted extensively from without first obtaining permission in writing from the copyright holder(s). The content must not be changed in any way or sold commercially in any format or medium without the formal permission of the copyright holders.



# Tuning the electronic properties of C12A7 via Sn doping and encapsulation

Navaratnarajah Kuganathan<sup>1,2,\*</sup>  and Alexander Chroneos<sup>1,2,\*</sup>

<sup>1</sup>Department of Materials, Imperial College London, London SW7 2AZ, UK

<sup>2</sup>Faculty of Engineering, Environment and Computing, Coventry University, Priory Street, Coventry CV1 5FB, UK

Received: 9 June 2020

Accepted: 8 October 2020

© The Author(s) 2020

## ABSTRACT

Cation doping in electride materials has been recently considered as a viable engineering strategy to enhance the electron concentration. Here we apply density functional theory-based energy minimisation techniques to investigate the thermodynamical stability and the electronic structures of Sn-doped and Sn-encapsulated in stoichiometric and electride forms of C12A7. The present calculations reveal that encapsulation is exoergic and doping is endoergic. The electride form is more energetically favourable than the stoichiometric form for both encapsulation and doping. Encapsulation in the electride results a significant electron transfer (1.52 |e|) from the cages consisting of extra-framework electrons to the Sn atom. The Sn forms almost + 4 state in the doped configuration in the stoichiometric form as reported for the electride form in the experiment. Similar charge state for the Sn is expected for the electride form though the extra-framework electrons localised on the Sn. Resultant complexes of both forms are magnetic. Whilst significant Fermi energy shift is noted for the doping in C12A7:O<sup>2-</sup> (by 1.60 eV) towards the conduction band, there is a very small shift (0.04 eV) is observed in C12A7:e<sup>-</sup>. Future experimental study on the encapsulation of Sn in both forms of C12A7 and doping of Sn in the stoichiometric form can use this information to interpret their experimental data.

## 1 Introduction

Rapid advancement of the electronic technologies necessitates the development of novel functional materials with cheap, non-hazardous, electronically conductive and tunable characteristics for the enhancement of electronic properties. In recent years, there has been a growing interest in inorganic electride materials because of their promising

applications in electronics due to their low work function and good electronic conductivity [1–7]. As there are chemically independent electrons occupied in electrides, it is expected that they can be used as electron emitters, superconductors and catalysts for different reactions including depletion of CO<sub>2</sub> and activation of N<sub>2</sub> [8–12]. Various stable inorganic electrides such as C12A7 [1, 13] and Ca<sub>2</sub>N [14] have been reported in the literature. Based on the nature of

Address correspondence to E-mail: n.kuganathan@imperial.ac.uk; ad0636@coventry.ac.uk

electron localisation they are classified as zero-dimensional (electrons localising in cavities) [15], one-dimensional (electrons localising in a channel) [16] and two-dimensional (electrons confining in a layer) [17]. Due to the potential uses of electrides in solid-state physics, there has been a significant interest to discover new electride materials or tailor the currently available electrides to tune their properties.

12CaO·7Al<sub>2</sub>O<sub>3</sub> (C12A7) [1, 12, 13] is a sub-nanoporous inorganic complex oxide mainly found in aluminous cement. It has a positively charged framework  $\{(Ca_{24}Al_{28}O_{64})^{4+}\}$  (consisting of twelve nanocages per unit cell) that is compensated by extra-framework anions. When the framework is compensated by two O<sup>2-</sup> ions, the resultant complex takes its stoichiometric form and is represented as  $[Ca_{24}Al_{28}O_{64}]^{4+} \cdot (O^{2-})_2$  {C12A7:O<sup>2-</sup>} [18]. Appropriate reduction treatment replaces those two extra-framework O<sup>2-</sup> ions with four electrons and the resultant complex takes its electride form with chemical formula of  $[Ca_{24}Al_{28}O_{64}]^{4+} \cdot (e^-)_4$  {C12A7:e<sup>-</sup>}<sup>1</sup>. As these four extra-framework electrons localise in the cages, this electride is classified as zero-dimensional. Extra-framework electrons have been replaced by a number of anions including F<sup>-</sup> [19], NH<sub>2</sub><sup>-</sup> [20], Cl<sup>-</sup> [19], S<sup>2-</sup> [21] and OH<sup>-</sup> [22]. Stabilisation of 12CaO·7Al<sub>2</sub>O<sub>3</sub> by incorporating O<sup>2-</sup>, F<sup>-</sup>, Cl<sup>-</sup>, S<sup>2-</sup> ions has been discussed by Zhmoidin and Chatterjee [21]. Thermodynamics and kinetics of hydroxide (OH<sup>-</sup>) ions inside the cages of 12CaO·7Al<sub>2</sub>O<sub>3</sub> (C12A7) were studied and it was concluded that the rate-determining is inward diffusion of OH<sup>-</sup> ions [22]. Encapsulation of NH<sub>2</sub><sup>-</sup> and H<sup>-</sup>, as well as NH<sub>2</sub><sup>2-</sup> was considered by Hayashi et al. [20] and it was found that C<sub>12</sub>A<sub>7</sub>:NH<sub>2</sub><sup>2-</sup> acts as a reactive nitrogen source for nitrogen transfer reactions. Furthermore, a variety of transition metals including Au [23] have been incorporated into C12A7:e<sup>-</sup> to optimise its catalytic activity and use as a storage material.

Cationic doping has been recently considered as an efficient strategy to modify the electronic properties of C12A7:e<sup>-</sup> for its use in electro catalysis and oxygen reduction reactions. Khan et al. [24] recently synthesised Sn-doped C12A7:e<sup>-</sup> and concluded that doped composite exhibited a long-time stability and methanol resistance during the oxygen reduction reaction that can be used in fuel cells. Very recently, Hu et al. [25] synthesised Sn-doped C12A7:e<sup>-</sup> using sol-gel method and observed that Sn was in the form of Sn<sup>4+</sup> in the doped composite and the electronic

configurations of Al and Ca were unaltered. Nevertheless, there are no theoretical studies that consider the experimental observation and calculate the electronic structures, thermodynamical stability and chemical states of doped-Sn.

In the present study, we employ density functional theory (DFT) simulations on a single Sn atom encapsulated and doped in both stoichiometric and electride forms of C12A7. The aim is to provide insights into thermodynamic stability, relaxed structures of encapsulated and doped C12A7, electron transfer between the Sn and C12A7, magnetic behaviour and electronic structures of resultant complexes.

## 2 Computational methods

Electronic structure calculations were performed on a single Sn atom encapsulated and doped in C12A7. We used a plane wave based DFT code VASP (Vienna Ab initio Simulation Package) [26, 27], which solves the standard Kohn–Sham (KS) equations using plane waves as basis sets. The exchange–correlation term was modelled using generalized gradient approximation (GGA) as parameterised by Perdew, Burke, and Ernzerhof, PBE [28]. Conjugate gradient algorithm [29] was used to optimise the structures. Forces on the atoms were calculated using the Hellmann–Feynman theorem including Pulay corrections. In all relaxed configurations, forces on the atoms were less than 0.001 eV/Å. A plane-wave basis set with a cut-off value of 500 eV and a 2 × 2 × 2 Monkhorst–Pack [30] *k*-point mesh were used in all calculations. Encapsulation energy for a single Sn atom in C12A7:O<sup>2-</sup> was calculated using the following equation:

$$E_{\text{Enc}} = E_{(\text{Sn}@C12A7:O^{2-})} - E_{(C12A7:O^{2-})} - E_{(\text{Sn})}, \quad (1)$$

where  $E_{(\text{Sn}@C12A7:O^{2-})}$  is the total energy of a single Sn atom encapsulated in C12A7:O<sup>2-</sup>,  $E_{(C12A7:O^{2-})}$  is the total energy of bulk C12A7:O<sup>2-</sup> and  $E_{(\text{Sn})}$  is the energy of an isolated gas phase Sn atom.

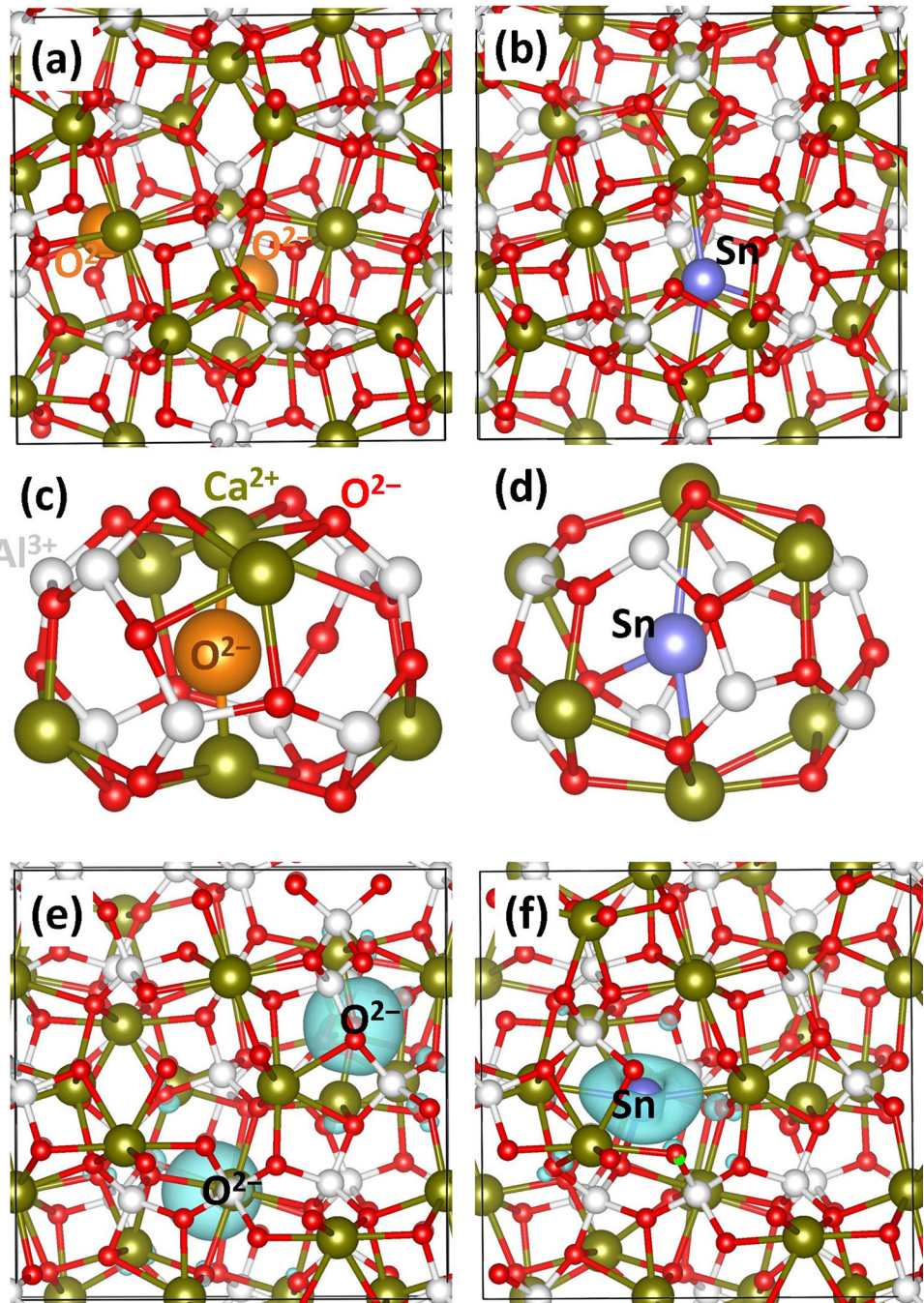
Substitution energy for a single Sn atom to replace a single Al atom in C12A7:O<sup>2-</sup> was calculated using the following equation:

$$E_{\text{Sub}} = E_{(\text{Sn}:C12A7:O^{2-})} + E_{(\text{Al})} - E_{(+C12A7:O^{2-})} - E_{(\text{Sn})}, \quad (2)$$

where  $E_{(\text{Sn};\text{C12A7};\text{O}^{2-})}$  is the total energy of a single Sn atom substituted on the Al site in  $\text{C12A7};\text{O}^{2-}$ ,  $E_{(\text{C12A7};\text{O}^{2-})}$  is the total energy of bulk  $\text{C12A7};\text{O}^{2-}$  and  $E_{(\text{Sn})}$  is the energy of an isolated gas phase Sn atom.

Encapsulation and substitution energies with respect to bulk Sn were also calculated and reported. The van der Waals (vdW) interactions were included in all calculations as parameterised by Grimme et al. [31]

**Fig. 1** Relaxed structures of **a**  $\text{C12A7};\text{O}^{2-}$  bulk, **b** Sn-encapsulated  $\text{C12A7};\text{O}^{2-}$ , **c** a cage occupied by extra-framework  $\text{O}^{2-}$  ion, **d** a cage occupied by encapsulated Sn and **e** and **f** constant charge density plots of extra-framework  $\text{O}^{2-}$  and Sn atom, respectively



### 3 Results and discussion

#### 3.1 Calculation of bulk C12A7

“Mayenite” type  $12\text{CaO}\cdot 7\text{Al}_2\text{O}_3$  (C12A7) belongs to the body-centred cubic lattice (space group  $I\bar{4}3d$ ) (see Fig. 1a) [18]. Its experimental lattice parameters were reported to be  $a = b = c = 11.99 \text{ \AA}$  and  $\alpha = \beta = \gamma = 90^\circ$  [18]. There are 12 cages present in a unit cell. In

the stoichiometric form of C12A7 (C12A7:O<sup>2-</sup>), two cages are occupied by O<sup>2-</sup> ions (see Fig. 1a). In the electrified form (C12A7:e<sup>-</sup>), there are four electrons present in a unit cell. In order to determine the equilibrium lattice constants, we performed energy minimisation calculations under constant pressure. This allowed us to relax the ionic positions and cell parameters. Calculated lattice parameters ( $a = 12.04 \text{ \AA}$ ,  $b = c = 12.01 \text{ \AA}$ ,  $\alpha = 90.02^\circ$ ,  $\beta = 89.95^\circ$ ,  $\gamma = 89.93^\circ$ ) in this simulation were in good agreement with those reported in the experiment and previous theoretical studies [32].

### 3.2 Encapsulation of a single Sn atom in C12A7:O<sup>2-</sup>

First we considered the encapsulation of a single Sn atom in C12A7:O<sup>2-</sup>. The relaxed structure and the cage occupied by the Sn are shown in Fig. 1. The position of the Sn is slightly off-centre and it forms bonds with cage wall oxygen and cage pole calcium ions. Table 1 reports the encapsulation energy calculated using a gas phase Sn atom as reference, Bader charge [33] on the encapsulated Sn atom, net magnetic moments, bond distances, volumes and Fermi energies of the relaxed configurations of both C12A7:O<sup>2-</sup> and Sn-encapsulated C12A7:O<sup>2-</sup>. Encapsulation energy is calculated to be  $-0.68 \text{ eV}$  meaning that the Sn atom is more stable than its isolated gaseous form. Bader charge analysis shows that there is a small electron transfer from the Sn to the lattice. The encapsulated structure becomes magnetic because of the unaltered outer electronic configuration of Sn ( $s^2p^2$ ) in which  $s$  electrons are paired and  $p$  electrons are unpaired. The magnetic moment of C12A7:O<sup>2-</sup> is 0. Two unpaired electrons on the Sn turn the resultant configuration magnetic with the magnetic moment of 2.00. The calculated Sn–O and Sn–Ca bond distances are 2.39 Å and 3.02 Å respectively showing the

**Fig. 2** **a** Total DOS plot of C12A7:O<sup>2-</sup>, **b** atomic DOS of extra-framework O<sup>2-</sup> ion in C12A7:O<sup>2-</sup>, **c** total DOS plot of Sn@C12A7:O<sup>2-</sup>, and **d** and **e** atomic DOSs of O<sup>2-</sup> ion and Sn in Sn@C12A7:O<sup>2-</sup>, respectively

interaction of the Sn with the lattice. This is also consistent with the exoergic encapsulation energy. Encapsulation has a very small effect (+ 0.1%) on the volume (refer to Table 1). Fermi energy has been shifted by  $\sim 1 \text{ eV}$  towards the conduction band upon encapsulation (see Fig. 2).

Density of states (DOSs) plots are shown in Fig. 2. Current simulations as reported in the previous simulations confirm that the C12A7:O<sup>2-</sup> is a wide-gap insulator. Additional gap states belonging to the Sn are introduced between the valence and conduction bands. This is further confirmed by the atomic DOS shown in Fig. 2.

### 3.3 Encapsulation of a single Sn atom in C12A7:e<sup>-</sup>

Next we encapsulated a single Sn atom into an empty cage in C12A7:e<sup>-</sup>. Figure 1a and b show the relaxed structures of C12A7:e<sup>-</sup> bulk and Sn-encapsulated C12A7:e<sup>-</sup>, respectively. In the relaxed structure, the Sn atom occupies the centre of the cage (see Fig. 1d) forming bonds with cage pole Ca ions. This is because of the charge ( $-1.52 |e|$ ) transferred from extra-framework electrons to the Sn (see Table 2) and the negatively charged Sn electrostatically attracted by two cage pole Ca<sup>2+</sup> ions. This is further confirmed by the exothermic encapsulation energy of  $-3.04 \text{ eV}$ . Notably, there is an enhancement in the encapsulation (by  $\sim 2.40 \text{ eV}$ ) by the electrified form compared to its stoichiometric form. Strong encapsulation is due to the donation of extra-framework electrons to the Sn. Charge density plots associated with the

**Table 1** Encapsulation energy, Bader charge on the Sn atom, magnetic moments, bond distances, volumes and the Fermi energies of C12A7:O<sup>2-</sup> and Sn-encapsulated C12A7:O<sup>2-</sup> (Sn@C12A7:O<sup>2-</sup>)

System	Encapsulation energy (eV)	Bader charge on Sn ( e )	Magnetic moment ( $\mu$ )	Sn–O (Å)	Sn–Ca (Å)	Volume (Å <sup>3</sup> )	Fermi energy (eV)
Sn@C12A7:O <sup>2-</sup>	$-0.68$ (2.68)	$+0.27$	2.00	2.39	3.02	1740.46	4.24
C12A7:O <sup>2-</sup>	–	–	0.00	–	–	1738.66	3.26

Encapsulation energy calculated using Sn bulk as a reference is provided in parenthesis

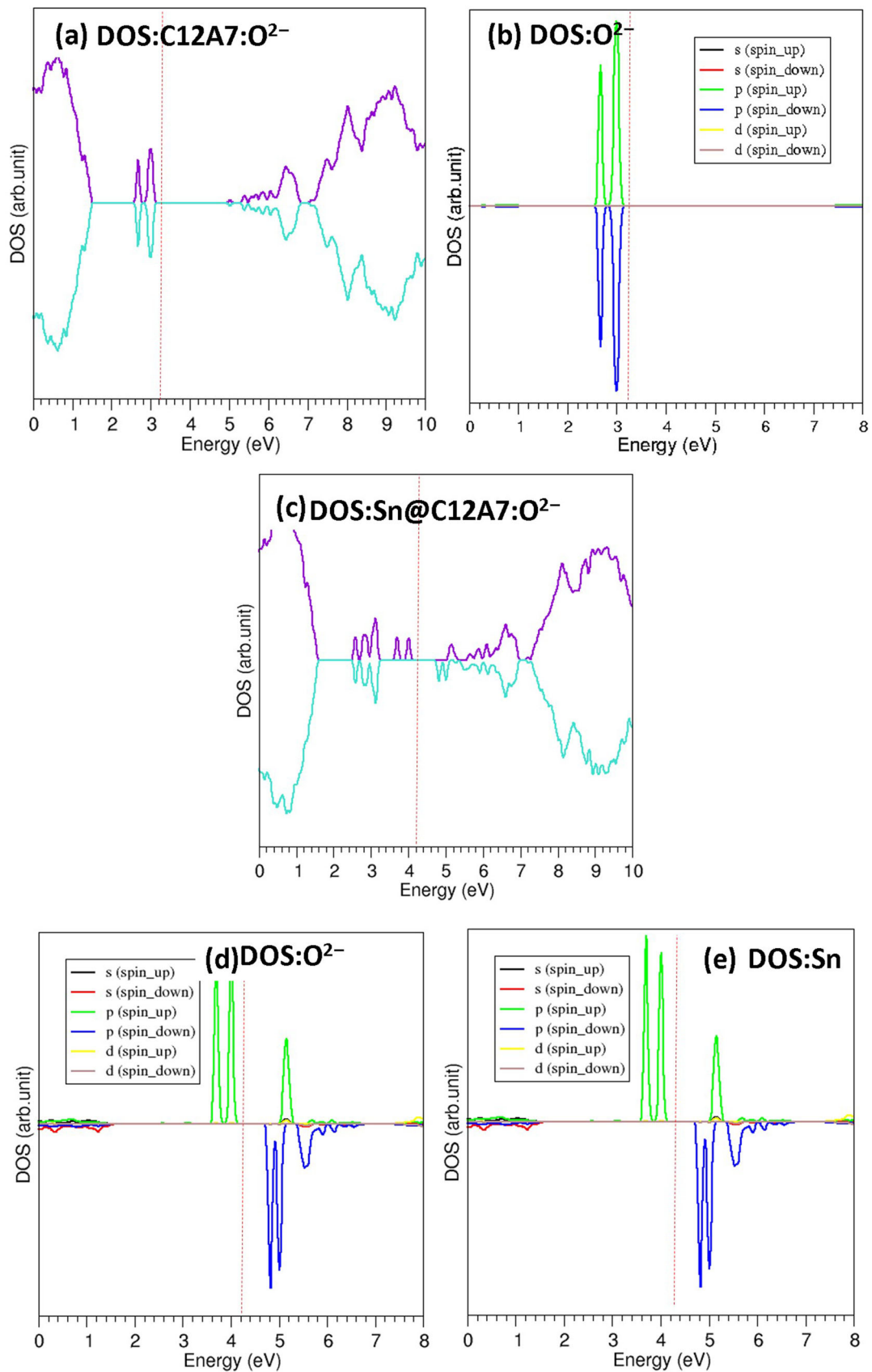
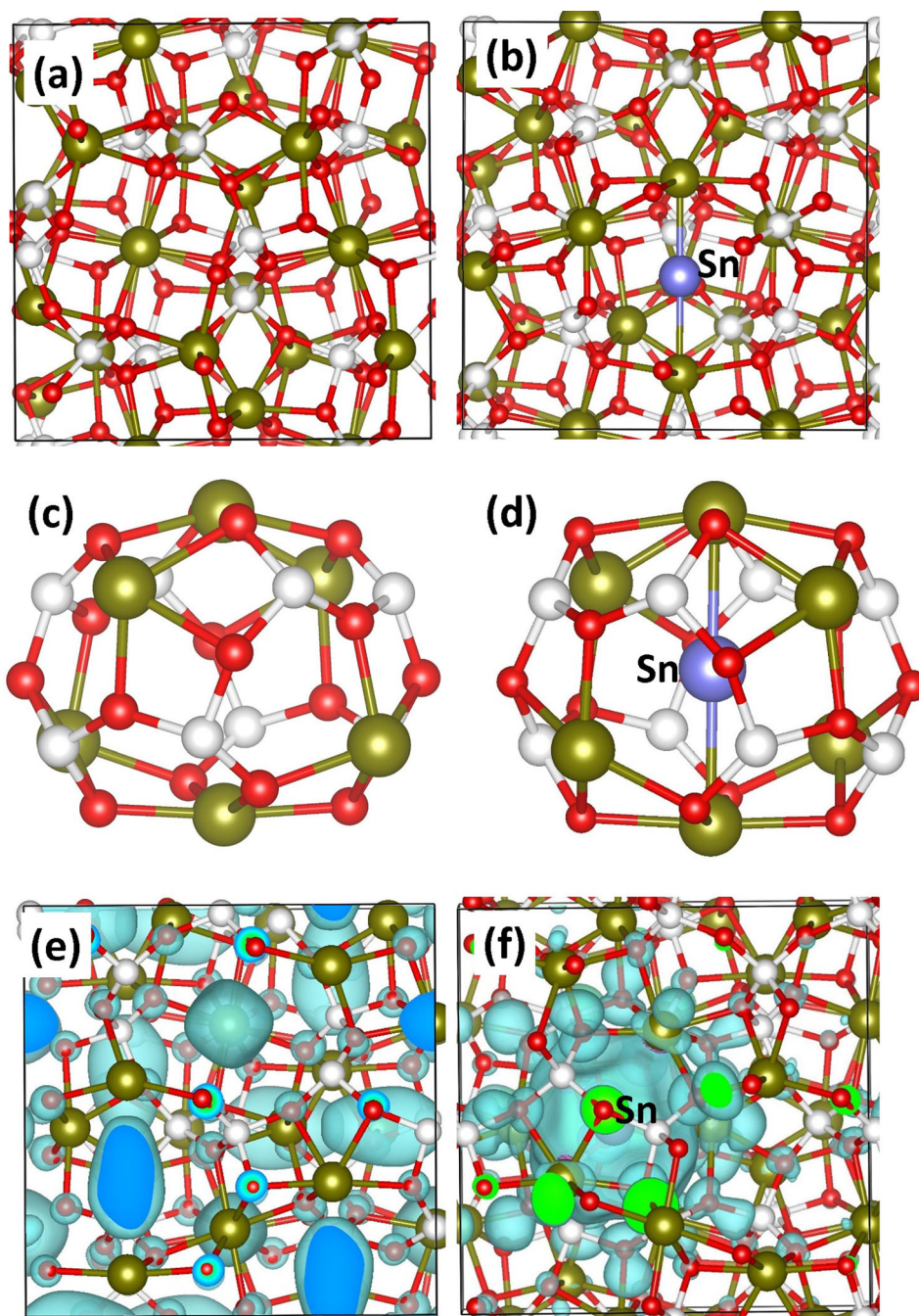


**Table 2** Encapsulation energy, Bader charge on the Sn atom, magnetic moments, bond distances, volumes and the Fermi energies of C12A7:e<sup>-</sup> and Sn-encapsulated C12A7:e<sup>-</sup> (Sn@C12A7:e<sup>-</sup>)

System	Encapsulation energy (eV)	Bader charge on Sn ( e )	Magnetic moment ( $\mu$ )	Sn–O (Å)	Sn–Ca (Å)	Volume (Å <sup>3</sup> )	Fermi energy (eV)
Sn@C12A7:e <sup>-</sup>	- 3.04 (0.32)	- 1.52	0.20	3.46	2.92	1759.08	5.18
C12A7:e <sup>-</sup>	-	-	0.00	-	-	1752.51	5.42

Encapsulation energy calculated using Sn bulk as a reference is provided in parenthesis

**Fig. 3** Relaxed structures of **a** C12A7:e<sup>-</sup> bulk, **b** Sn-encapsulated C12A7:e<sup>-</sup>, **c** a cage occupied by extra-framework electron ( $\frac{1}{3}$  e<sup>-</sup>) and **d** a cage occupied by encapsulated Sn; constant charge density plots of **e** extra-framework electrons and **f** Sn atom



extra-framework electrons in C12A7:e<sup>-</sup> and Sn-encapsulated C12A7:e<sup>-</sup> are shown in Fig. 2. Encapsulation of Sn has reduced the extra-framework electrons by 1.52. A small net magnetic moment is observed in the resultant complex. A small volume expansion (+ 0.37%) is observed upon encapsulation. The Fermi energy is shifted slightly by 0.24 eV towards the valence band (Fig. 3).

C12A7 containing extra-framework electrons (i.e. C12A7:e<sup>-</sup>) is metallic according to our calculations and previous simulations [32, 34] (see Fig. 4a). Sn-doped C12A7:e<sup>-</sup> also exhibits metallic character. Additional peak arising from *p* states of Sn appears near the Fermi energy level.

### 3.4 Doping of a single Sn atom on the Al site in C12A7:O<sup>2-</sup>

Here we substitute a single Sn atom on the Al site in C12A7:O<sup>2-</sup>. Figure 5 shows the relaxed structures including the cage containing Sn atom. The substitution energy is calculated to be 5.37 eV suggesting that the Al–O bond is stronger than the Sn–O bond. This is further supported by the shorter Al–O bond length (1.75 Å) than Sn–O bond length (2.01–2.28 Å). Bader charge analysis shows that the charges of the Al ion in the un-doped C12A7:O<sup>2-</sup> and the Sn are + 3 and + 3.60, respectively. This means that additional 0.60 electrons has been transferred by the Sn to the lattice. This in turns constitutes the resultant complex metallic according to the DOS plots (Fig. 5d–f). Figure 5c shows the charge density of additional electrons localised in the lattice. The present calculations further confirm that Sn is in the form of Sn<sup>4+</sup>

according the Bader charge analysis. This is in agreement with the experimental results for C12A7:e<sup>-</sup> carried out by Hu et al. [25] though they have not tested for C12A7:O<sup>2-</sup>. The <sup>119</sup>Sn Mössbauer spectroscopy can also be used to determine the oxidation number of Sn atoms.

The net magnetic moment is calculated to be 0.78μ indicating that resultant complex is magnetic (see Table 3). This is due to the electrons released by the Sn to the lattice. A small expansion of volume (0.54%) is observed upon Sn doping. The Fermi energy increases significantly by 1.60 eV towards conduction band due to the Sn impurity which gives electrons to the system.

### 3.5 Doping of a single Sn atom on the Al site in C12A7:e<sup>-</sup>

Finally, the electrider form of C12A7 was considered for substitution. Figure 6 shows the relaxed structures of Sn-doped C12A7:e<sup>-</sup> and cage showing doped-Sn, constant charge density plot associated with the extra-framework electrons after doping, total DOS plot and atomic DOS plot of Sn. Substitution energy is calculated to be 3.58 eV showing that doping is endothermic process due to the stronger Al–O bond (bond distance = 1.75 Å) than Sn–O bond (bond distance = 2.22–2.43 Å). Doping of Sn in C12A7:e<sup>-</sup> is 1.79 eV more favourable than in C12A7:O<sup>2-</sup>. This is due to the stabilisation of positive charge on the Sn atom by the negatively charged extra-framework electrons. Bader charge analysis shows that the overall charge on the Sn atom is + 1.60. This does not mean that the doped-Sn lost

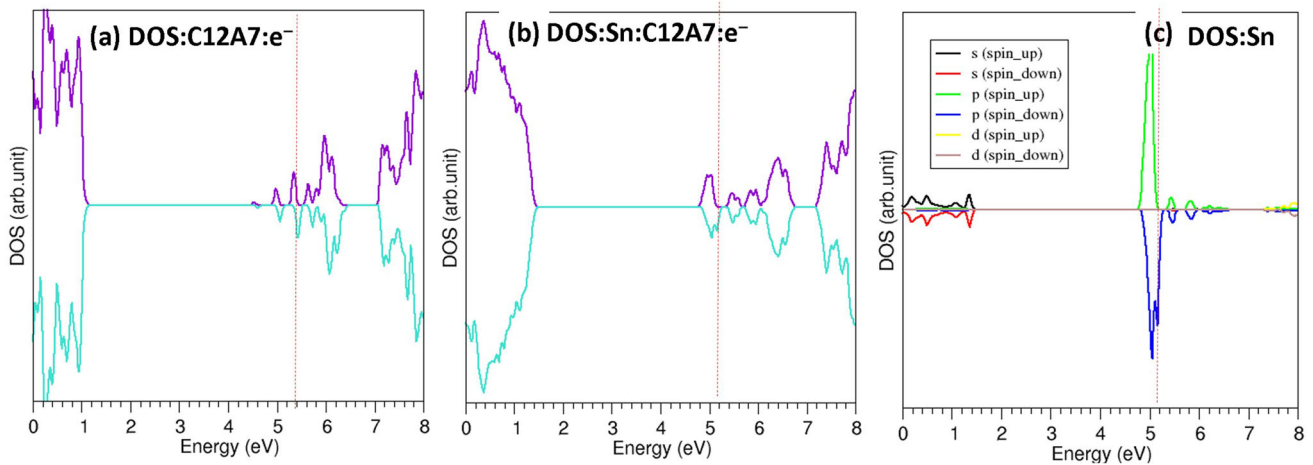


**Fig. 4** **a** Total DOS plot of C12A7:e<sup>-</sup>, **b** total DOS plot of Sn@C12A7:e<sup>-</sup> and **c** atomic DOSs of Sn in Sn@C12A7:e<sup>-</sup>



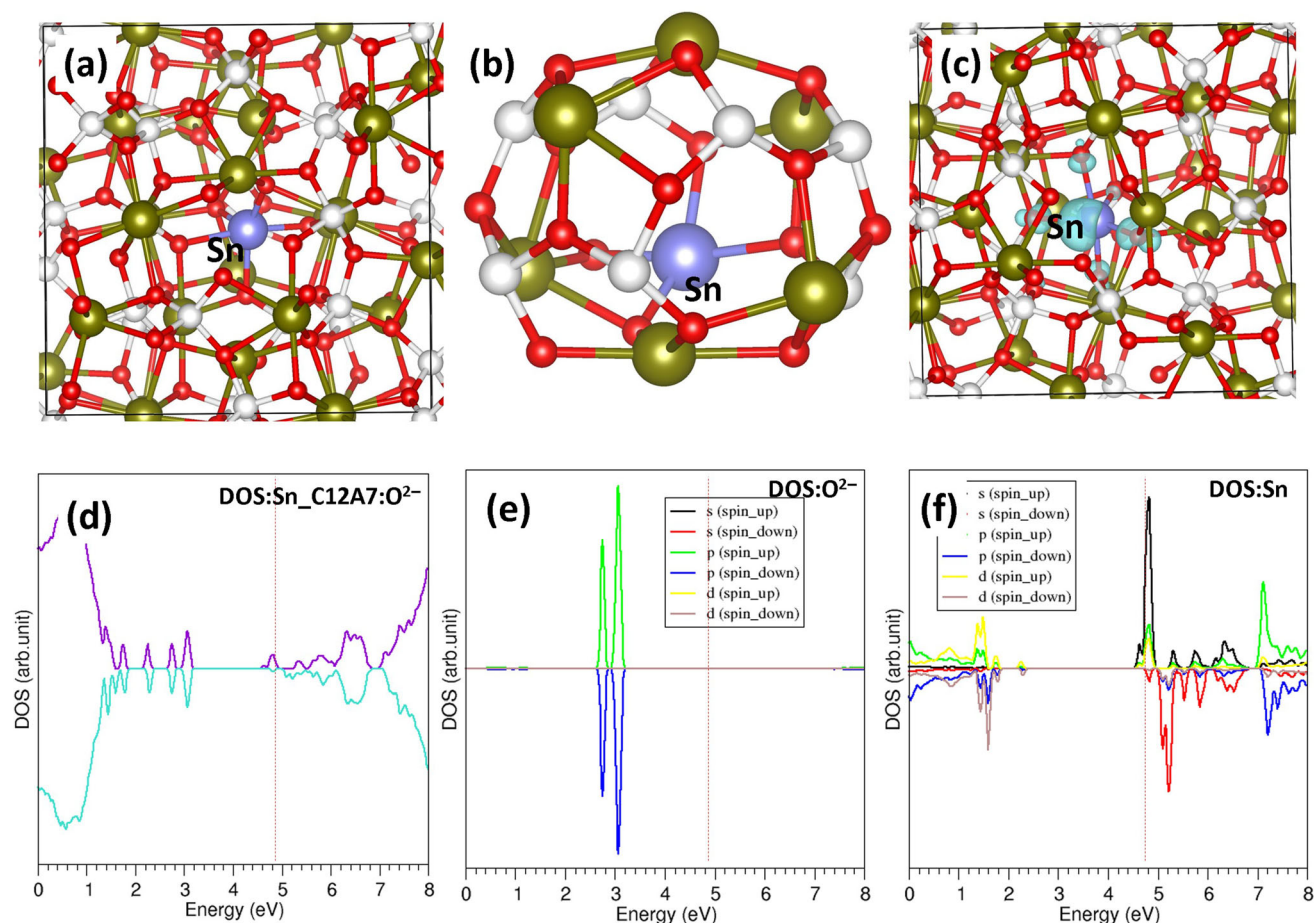


**Fig. 5** **a** Relaxed structure of Sn-doped C12A7:O<sup>2-</sup>, **b** cage showing substituted Sn, **c** constant charge density plot showing the electrons introduced by the doping, **d** total DOS plot of Sn.C12A7:O<sup>2-</sup> and **e** and **f** atomic DOS plots of O<sup>2-</sup> and Sn, respectively

**Table 3** Substitution energy, Bader charge on the Sn atom, magnetic moments, bond distances, volumes and the Fermi energies of C12A7:O<sup>2-</sup> and Sn-doped C12A7:O<sup>2-</sup> (Sn.C12A7:O<sup>2-</sup>)

System	Substitution energy (eV)	Bader charge on Sn ( e )	Magnetic moment ( $\mu$ )	Sn–O (Å)	Sn–Ca (Å)	Volume (Å <sup>3</sup> )	Fermi energy (eV)
Sn.C12A7:O <sup>2-</sup>	5.37 (8.73)	+ 3.60	0.78	2.01–2.28	–	1748.11	4.86
C12A7:O <sup>2-</sup>	–	–	0.00	–	–	1738.66	3.26

Substitution energy calculated using Sn bulk as a reference is provided in parenthesis

only 1.60 electrons. We assume that the Sn lost  $\sim$  3.60 electron as it did in C12A7:O<sup>2-</sup> and the low net positive charge on the Sn is due to the extra-frame work electrons delocalised in the lattice. This is further confirmed by the net magnetic moment of  $0.85 \mu$  and the localisation of some electrons on the Sn atom (see Fig. 6c). A negligible volume change of 0.32% is

observed. The Fermi energy changes slightly by 0.06 eV towards valence band (Table 4).

## 4 Conclusions

In conclusion, we examined the efficacy of encapsulating and doping of a single Sn atom into the stoichiometric and electride forms of C12A7 using spin-

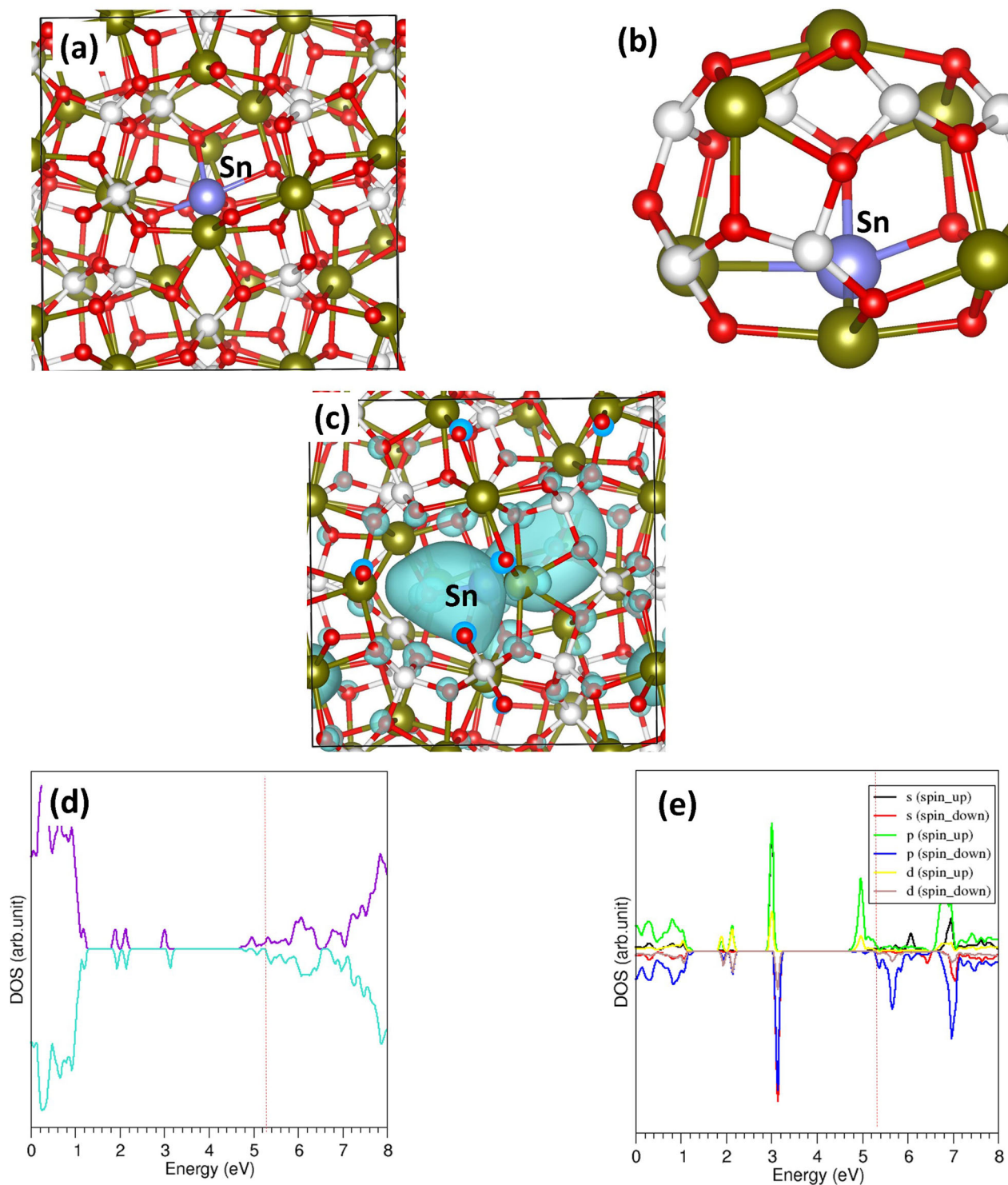


**Fig. 6** **a** Relaxed structure of Sn-doped C12A7:e<sup>-</sup>, **b** cage showing substituted Sn, **c** constant charge density plot showing the electron distribution after doping, **d** total DOS plot of Sn.C12A7:e<sup>-</sup>, and **e** atomic DOS plots of Sn

polarised DFT together with dispersion. The calculations show that both forms of C12A7 exoergically encapsulate the Sn atom. The electride form exhibits

an enhancement (by 2.36 eV) to encapsulate the atom due to the significant electron transfer (1.52 |e|) between extra-framework electrons and the Sn atom.

**Table 4** Substitution energy, Bader charge on the Sn atom, magnetic moments, bond distances, volumes and the Fermi energies of C12A7:e<sup>-</sup> and Sn-doped C12A7:e<sup>-</sup> (Sn.C12A7:e<sup>-</sup>) structures

System	Substitution energy (eV)	Bader charge on Sn ( e )	Magnetic moment ( $\mu$ )	Sn–O (Å)	Sn–Ca (Å)	Volume (Å <sup>3</sup> )	Fermi energy (eV)
Sn.C12A7:e <sup>-</sup>	3.58 (6.94)	+ 1.60	0.85	2.22–2.43	–	1758.13	5.36
C12A7:e <sup>-</sup>	–	–	0.00	–	–	1752.51	5.42

Substitution energy calculated using Sn bulk as a reference is provided in parenthesis

Both encapsulated complexes are magnetic. Whilst there is a significant change ( $\sim 1$  eV towards conduction band) in the Fermi energy for C12A7:O<sup>2-</sup> only a small change (0.26 eV towards valence band) is noted for C12A7:e<sup>-</sup>.

Doping is endoergic in both forms of C12A7, however, the electrified form is more energetically favourable (by 1.80 eV) for the doping process than that of stoichiometric form. In the stoichiometric form, the Sn forms almost + 4 state releasing some electrons to the cage. The electrified form reduces the charge on the Sn atom due to the extra-framework electrons. Nevertheless, it is expected that similar charge state is formed for the Sn in the electrified form as well. This observation is in agreement with the experiment. Resultant complexes are magnetic in both cases. Doping in C12A7:O<sup>2-</sup> has increased the Fermi energy by 1.60 eV towards the conduction band. Fermi energy is almost unaltered ( $\sim$  by 0.04 eV) up on doping in C12A7:e<sup>-</sup>. Current simulation study provides a detail information regarding the stability, electron transfer, magnetic behaviour and electronic structures of Sn-encapsulated and Sn-doped C12A7. We anticipate that future experimental study can use this information to interpret their experimental data.

## Acknowledgements

High Performance Computing Centre at Imperial College London is acknowledged for providing computational facilities and support.

**Open Access** This article is licensed under a Creative Commons Attribution 4.0 International License, which permits use, sharing, adaptation, distribution and reproduction in any medium or format, as long as you give appropriate credit to the original author(s) and the source, provide a link to the

Creative Commons licence, and indicate if changes were made. The images or other third party material in this article are included in the article's Creative Commons licence, unless indicated otherwise in a credit line to the material. If material is not included in the article's Creative Commons licence and your intended use is not permitted by statutory regulation or exceeds the permitted use, you will need to obtain permission directly from the copyright holder. To view a copy of this licence, visit <http://creativecommons.org/licenses/by/4.0/>.

## References

- 1 S. Matsuishi, Y. Toda, M. Miyakawa, K. Hayashi, T. Kamiya, M. Hirano, I. Tanaka, H. Hosono, *Science* **301**, 626 (2003)
- 2 M. Hirayama, S. Matsuishi, H. Hosono, S. Murakami, *Phys. Rev. X* **8**, 031067 (2018)
- 3 K. Khan, A.K. Tareen, M. Aslam, K.H. Thebo, U. Khan, R. Wang, S.S. Shams, Z. Han, Z. Ouyang, *Prog. Solid State Chem.* **54**, 1 (2019)
- 4 Z. Li, J. Yang, J.G. Hou, Q. Zhu, *Chem. Eur. J.* **10**, 1592 (2004)
- 5 M.J. Wagner, J.L. Dye, *Annu. Rev. Mater. Sci.* **23**, 223 (1993)
- 6 M.C. Barry, Z. Yan, M. Yoon, S.R. Kalidindi, S. Kumar, *Appl. Phys. Lett.* **113**, 131902 (2018)
- 7 M.S. Anderson, *Appl. Phys. Lett.* **103**, 131103 (2013)
- 8 D.L. Druffel, K.L. Kuntz, A.H. Woerner, F.M. Alcorn, J. Hu, C.L. Donley, S.C. Warren, *J. Am. Chem. Soc.* **138**, 16089 (2016)
- 9 Y. Toda, H. Hirayama, N. Kuganathan, A. Torrisi, P.V. Sushko, H. Hosono, *Nat. Commun.* **4**, 2378 (2013)
- 10 M. Kitano, S. Kanbara, Y. Inoue, N. Kuganathan, P.V. Sushko, T. Yokoyama, M. Hara, H. Hosono, *Nat. Commun.* **6**, 6731 (2015)
- 11 T.-N. Ye, Z. Xiao, J. Li, Y. Gong, H. Abe, Y. Niwa, M. Sasase, M. Kitano, H. Hosono, *Nat. Commun.* **11**, 1020 (2020)

- 12 H. Hosono, S.-W. Kim, S. Matsuishi, S. Tanaka, A. Miyake, T. Kagayama, K. Shimizu, *Philos. Trans. R. Soc. A* **373**, 20140450 (2015)
- 13 S. Watauchi, I. Tanaka, K. Hayashi, M. Hirano, H. Hosono, *J. Cryst. Growth* **237–239**, 801 (2002)
- 14 K. Lee, S.W. Kim, Y. Toda, S. Matsuishi, H. Hosono, *Nature* **494**, 336 (2013)
- 15 Y. Tsuji, P.L.V.K. Dasari, S.F. Elatresh, R. Hoffmann, N.W. Ashcroft, *J. Am. Chem. Soc.* **138**, 14108 (2016)
- 16 Y. Zhang, Z. Xiao, T. Kamiya, H. Hosono, *J. Phys. Chem. Lett.* **6**, 4966 (2015)
- 17 T. Tada, S. Takemoto, S. Matsuishi, H. Hosono, *Inorg. Chem.* **53**, 10347 (2014)
- 18 J.A. Imlach, L.S. Dent Glasser, F.P. Glasser, *Cem. Concr. Res.* **1**, 57 (1971)
- 19 J. Jeevaratnam, F.P. Glasser, L.S.D. Glasser, *J. Am. Ceram. Soc.* **47**, 105 (1964)
- 20 F. Hayashi, Y. Tomota, M. Kitano, Y. Toda, T. Yokoyama, H. Hosono, *J. Am. Chem. Soc.* **136**, 11698 (2014)
- 21 G.I. Zhmoidin, A.K. Chatterjee, *Cem. Concr. Res.* **14**, 386 (1984)
- 22 K. Hayashi, M. Hirano, H. Hosono, *J. Phys. Chem. B* **109**, 11900 (2005)
- 23 M. Miyakawa, H. Kamioka, M. Hirano, T. Kamiya, P.V. Sushko, A.L. Shluger, N. Matsunami, H. Hosono, *Phys. Rev. B* **73**, 205108 (2006)
- 24 K. Khan, A. Khan Tareen, J. Li, U. Khan, A. Nairan, Y. Yuan, X. Zhang, M. Yang, Z. Ouyang, *Dalton Trans.* **47**, 13498 (2018)
- 25 Q. Hu, R. Tan, W. Yao, Y. Cui, J. Li, W. Song, *Appl. Surf. Sci.* **508**, 145244 (2020)
- 26 G. Kresse, J. Furthmüller, *Phys. Rev. B* **54**, 11169 (1996)
- 27 G. Kresse, D. Joubert, *Phys. Rev. B* **59**, 1758 (1999)
- 28 J.P. Perdew, K. Burke, M. Ernzerhof, *Phys. Rev. Lett.* **77**, 3865 (1996)
- 29 W.H. Press, S.A. Teukolsky, W.T. Vetterling, B.P. Flannery, *Numerical Recipes in C: The Art of Scientific Computing*, 2nd edn. (Cambridge University Press, Cambridge, 1992)
- 30 H.J. Monkhorst, J.D. Pack, *Phys. Rev. B* **13**, 5188 (1976)
- 31 S. Grimme, J. Antony, S. Ehrlich, H. Krieg, *J. Chem. Phys.* **132**, 154104 (2010)
- 32 N. Kuganathan, A. Chreneos, R.W. Grimes, *Sci. Rep.* **9**, 13612 (2019)
- 33 R.F.W. Bader, *Theor. Chem. Acc.* **105**, 276 (2001)
- 34 P.V. Sushko, A.L. Shluger, Y. Toda, M. Hirano, H. Hosono, *Proc. R. Soc. A* **467**, 2066 (2011)

**Publisher's Note** Springer Nature remains neutral with regard to jurisdictional claims in published maps and institutional affiliations.